Theoretical Investigation of the Inversion of the Methylcyclopropyl Radical†

Francesco Zerbetto,‡ Marek Z. Zgierski,* and Willem Siebrand

Contribution from the Division of Chemistry, National Research Council of Canada, Ottawa, Ontario, Canada K1A 0R6. *Received August 5, 1988*

Abstract: The dynamics of the inversion of the methylcyclopropyl radical is analyzed theoretically. Ab initio UHF calculations are carried out for a fully optimized geometry, and the vibrational force field is calculated at stationary points of the potential. The inversion is shown to involve not only the out-of-plane methyl vibration but also the methyl rotation, both subject to potential energy barriers. The inversion rate constant is calculated for temperatures ≥90 K where averaging over the methyl rotation is permitted. An analytical inversion potential, based on the calculated force field but adjusted empirically, is shown to account satisfactorily for the observed rate constants in the range 94 K ≤ T ≤ 160 K. Heavy-atom tunneling contributes substantially to the calculated inversion rate. At very low temperatures methyl torsion is predicted to slow down the inversion and to give rise to a significant deuterium effect.

1. Introduction

In a recent paper,[1] it was shown that the inversion of oxiranyl proceeds by tunneling: The rate of inversion, measured by ESR spectroscopy, exhibits a large primary kinetic isotope effect, and its temperature dependence shows a characteristic "curved" Arrhenius plot. This interpretation is supported by detailed quantum-chemical and dynamical calculations, which indicate that the observed rate parameters are in good agreement with theoretical results. The oxiranyl radical rather than the simpler cyclopropyl radical was chosen to study the inversion dynamics because the rate of inversion of cyclopropyl is too fast to be accessible by ESR techniques. In methylcyclopropyl, the inversion is slow enough to be monitored by ESR signals, but this reaction follows the usual Arrhenius plot and is not normally associated with tunneling.[2,3]

In the present paper, we take a closer look at this inversion. Although tunneling is obviously less important for a methyl group than for a proton or deuteron, it may not be prudent to neglect it entirely. A hint that the conventional over-the-barrier picture is not completely satisfactory is provided by the value of the preexponential factor found to be 2×10^{13} s^{-1}, which amounts to a transition frequency of about 330 cm^{-1}. This seems to be slightly high for the out-of-plane vibrational frequency at energies above the barrier. It therefore seems possible that at lower temperatures tunneling transitions well below the top of the barrier make a substantial contribution to the observed inversion rate. Since the ESR data[3] indicate fixed positions for methyl protons at 94 K, methyl rotation will be strongly hindered at this temperature. This suggests that the methyl out-of-plane vibration governing the inversion is coupled with methyl rotation.

Earlier ab initio calculations,[4,5] including full geometry optimization at the UHF/3-21 G level of theory,[6] indicate equilibrium configurations of C_h symmetry with a methylenic CH bond bisecting the plane of the ring. This would imply that inversion is accompanied by methyl rotation over 60°. However, no force field calculations are available nor has the orientation of the methyl group in the transition state been specified. The calculated pyramidalization angle of 43.4° differs sharply from the experimental estimate of 22.9°.[3]

For our purpose it will thus be necessary to carry out new calculations of the same type as those reported for oxiranyl.[1] Using an ab initio spin-unrestricted Hartree–Fock (UHF) method, we calculate the vibrational force field in the nonplanar equilibrium configurations and in the planar transition state between them. The resulting structural data will form the basis of an investigation of the dynamics of the inversion.

2. Computational Methods

The ab initio calculations were performed with the GAMESS program[7] at the UHF/6-31 G** level of theory.[8] The geometry was fully optimized, and the stationary points were characterized through the Hessian matrix. Expectation values of S^2 were calculated to check for contamination by higher spin states, which can occur in the UHF formalism. The resulting values were all ≤0.77 and thus close enough to the exact value of 0.75 to show that the method is suitable in the case at hand.

Table I. Energies E, Relative Energies ΔE, Zero-Point Energies ϵ_0, and Inversion Barrier Heights $\Delta\epsilon_0$ for Six Conformations of the Methylcyclopropyl Radical

conformn	E, hartree	ΔE, cm^{-1}	ϵ_0, cm^{-1}	$\Delta\epsilon_0$, cm^{-1}
C_h/bm	−155.469 32		22439	
C_h/e	−155.461 66	1681	22106	1495
C_h/bs	−155.461 65	1683	22156	1638
C_1/s	−155.461 65	1683	22087	1478
C_1/m	−155.469 29	7	22383	−49
C_h/mb	−155.466 66	584	22321	558

Table II. Structural Parameters for 1-Methylcyclopropyl[a]

	C_h/bm	C_h/e	C_h/bs	C_i/s	C_1/m	C_h/mb
C_1–C_2	1.469	1.454	1.456	1.455	1.469	1.467
C_1–C_3	1.469	1.455	1.456	1.454	1.469	1.467
C_1–C_4	1.489	1.483	1.484	1.483	1.490	1.497
C_4–H_5	1.091	1.085	1.090	1.089	1.091	1.087
C_4–H_6	1.085	1.089	1.086	1.087	1.085	1.086
C_4–H_7	1.085	1.089	1.086	1.085	1.085	1.086
C_2–H_8	1.078	1.081	1.081	1.081	1.079	1.078
C_3–H_{10}	1.078	1.081	1.081	1.081	1.079	1.078
C_2–H_9	1.080	1.081	1.081	1.081	1.078	1.080
C_3–H_{11}	1.080	1.081	1.081	1.081	1.078	1.080
$C_2C_1C_3$	62.38	63.63	63.62	63.61	62.33	63.33
$C_4C_1C_2C_3$	39.45	0.00	0.00	0.00	39.56	37.81
methyl rotation	90.00	180.00	90.00	74.13	85.75	270.00

[a] Bond lengths are in angstroms; angles are in degrees.

† Issued as NRCC No. 29475.
‡ NRCC Research Associate.

(1) Deycard, S.; Lusztyk, J.; Ingold, K. U.; Zerbetto, F.; Zgierski, M. Z.; Siebrand, W. *J. Am. Chem. Soc.* **1988**, *110*, 6721–6726.
(2) Johnston, L. J.; Ingold, K. U. *J. Am. Chem. Soc.* **1986**, *108*, 2343–2348.
(3) Deycard, S.; Hughes, L.; Lusztyk, J.; Ingold, K. U. *J. Am. Chem. Soc.* **1987**, *109*, 4954–4960.
(4) Dupuis, M.; Pacansky, J. *J. Chem. Phys.* **1982**, *76*, 2511–2515.
(5) Ellinger, J.; Subra, R.; Levy, B.; Millie, P.; Berthier, G. *J. Chem. Phys.* **1974**, *62*, 10–29.
(6) Lien, M. H.; Hopkins, A. C. *J. Comput. Chem.* **1985**, *6*, 274–281. Delbecq, F. *THEOCHEM* **1986**, *136*, 65–75.
(7) Dupuis, M.; Spangler, D.; Wendoloski, J. J. NRCC Software Catalogue Program QG01, 1980. Revised by: Schmidt, M. W.; Baldridge, K. K.; Boatz, J. A.; Koseki, S.; Gordon, M. S.; Elbert, S. T.; Lam, B. T. *QCPE* **1987**, *7*, 115.
(8) Francl, M. M.; Pietro, W. J.; Hehre, W. J.; Binkley, J. S.; Gordon, M. S.; De Frees, D. J.; Pople, J. A. *J. Chem. Phys.* **1982**, *77*, 3654–3665. Hariharan, P. C.; Pople, J. A. *Theor. Chim. Acta* **1973**, *28*, 213–222.

0002-7863/89/1511-2799$01.50/0 Published 1989 by the American Chemical Society

Table III. Calculated Normal-Mode Frequencies (in cm^{-1}) for 1-Methylcyclopropyl in the C_h/bm, C_h/bs, and C_h/mb Configurations

a′ symmetry				a″ symmetry			
	C_h/bm	C_h/bs	C_h/mb		C_h/bm	C_h/bs	C_h/mb
CH_2 stretch	3346	3309	3343	CH_2 stretch	3331	3294	3329
CH_2 stretch	3268	3231	3265	CH_{2eso} stretch	3264	3252	3235
CH_3 stretch	3234	3208	3161	CH_2 stretch	3262	3226	3259
CH_3 stretch	3165	3132	3219	CCH bend	1606	1614	1615
ring + CH_2 deformn	1649	1602	1647	CH_2 deformn	1589	1594	1591
CH_3 deformn	1614	1523	1609	CH_3 deformn + CCC ring	1272	1257	1277
CC_{eso} + C skeleton pyram	1549	1560	1547	CC_{eso} + CH_3 deformn	1230	1244	1217
CC stretch	1475	1669	1478	CC ring + CH_2 twist	1200	1208	1200
C skeleton pyram	1261	1117	1239	CC_{eso} + CCC_{endo}	988	1004	982
CH_2 wag	1163	1178	1158	CH_2 scissors	911	919	915
CCH bend + CCC ring				ring deformn	348	339	368
+CC ring	1076	1038	1034	CH_3 rotn	183	90*i*	188*i*
CCH bend	1012	1067	1064				
CH_2 twist	816	832	833				
CCC + CC ring	774	703	766				
C skeleton pyram	293	292i	290				

Table IV. Same as Table III but for the C_h/e Configuration

a′ symmetry		a″ symmetry	
assignt	C_h/e	assignt	C_h/e
CH stretch	3268	CH_2 stretch	3319
CH_2 stretch	3249	CH_2 stretch	3303
CH_2 stretch	3242	CH_2 methyl stretch	3207
CH_3 stretch	3164	CCH out-of-plane	1605
CC stretch	1668	CH_2 deformn	1257
CH_2-methyl deformn	1613	CCC + CH_2 deformn	1119
CH_2 deformn	1592	CH_2 methyl wag	1059
		C skeleton pyram	
CC stretch	1559	CH_2 scissors	923
CCH in plane + CC stretch	1520	CH_2 scissors	829
CCH (methyl) + CCC	1243	CH_3 rotn	94
CCC bend + CH_2 wag	1211	C skeleton pyram	298i
CH_2 wag	1182		
CC stretch + CH_2 wag	1038		
CCC bend + CCH (methyl)	1000		
CCC bend	708		
CCC bend	338		

Table V. Summary of the Normal-Mode Frequencies for Pyramidalization and Methyl Rotation (in cm^{-1})

conformn	pyrami-dalization	$-CH_3$ rotation	conformn	pyrami-dalization	$-CH_3$ rotation
C_h/bm	293	183	C_1/s	295*i*	36
C_h/e	298*i*	94	C_1/m	283	170
C_h/bs	292*i*	90*i*	C_h/mb	290	188i

To obtain insight in the overall shape of the potential energy surface, the following conformations were studied:

(i) C_h/bm, a conformation of C_h symmetry with an out-of-plane methyl carbon atom such that a methyl CH bond bisects the plane of the ring (Figure 1, top); (ii) C_h/e, a planar conformation of C_h symmetry with an in-plane methyl carbon atom such that a methyl CH bond eclipses the plane of the ring (Figure 2, top); (iii) C_h/bs, as (ii) except that a methyl CH bond bisects the plane of the ring (Figure 2, bottom); (iv) C_h/mb, as (i) except that the methyl group is rotated over 180° (or 60°), also referred to as the straddled conformation (Figure 1, bottom); (v) C_1/m, an asymmetric conformation with an out-of-plane methyl carbon atom; (vi) C_1/s, as (v) with an in-plane methyl carbon atom.

3. Computational Results

The results of the computations are listed in Tables I–V. In Table I, we collect the energies of conformations (i)–(vi). Table II lists structural parameters of all six conformations and Tables III and IV list normal mode frequencies for four conformations. Finally, in Table V, we list the frequencies associated with the methyl rotation and carbon skeleton pyramidalization (methyl out-of-plane bending) for all six conformations.

These results predict that the conformation C_h/bm will be the global minimum with C_h/e as the transition state between the two equivalent C_h/bm conformations. C_h/bs is a second-order saddle point, the associated Hessian of the electronic energy having two negative eigenvalues, viz. for methyl rotation and skeletal pyramidalization. C_h/bs has almost the same energy as C_h/e, which suggests the presence of a first-order saddle point of lower energy to be reached by methyl rotation. We obtained such a confor-

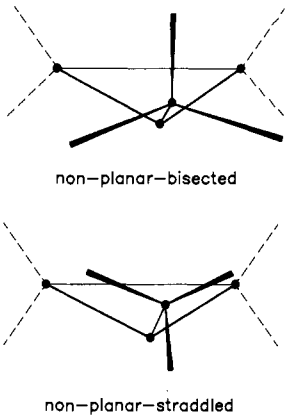

Figure 1. Conformations C_h/bm (top) and C_h/mb (bottom) of 1-methylcyclopropyl. C_h/mb differs from the stable C_h/bm conformation by a methyl rotation over 60°.

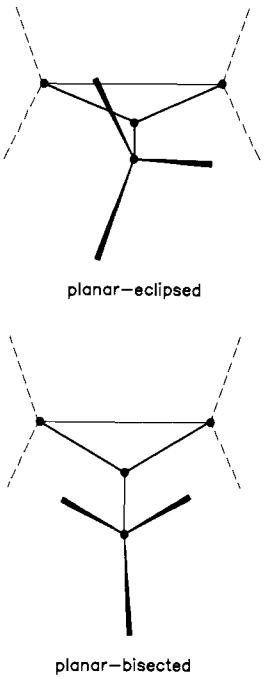

Figure 2. Conformations C_h/e (top) and C_h/bs (bottom) of 1-methylcyclopropyl. C_h/bs differs from the "transition state" C_h/e by a methyl rotation.

Table VI. Comparison of the Characteristics of the ab Initio and Empirical Potentials for the Methyl Inversion in Methylcyclopropyl

	frequency at the bottom, cm^{-1}	frequency at the top, cm^{-1}	pyramidalization angle, deg	barrier height, cm^{-1}
ab initio	293	292*i*	39.5	1495
empirical	290	290*i*	35.7	1250

mation by relieving the symmetry constraints, rotating the methyl group over 30°, and optimizing the geometry: it turned out to be isoenergetic with C_1/s before correction for zero-point energy differences and lower even than C_h/e after correction. Analogously, a second minimum was located. It therefore appears that there is a region of the potential energy surface where methyl rotation is essentially free, namely near the "planar" transition state. However, methyl rotation between the conformations C_h/bm and C_h/mb is hindered by a substantial barrier, in agreement with the experimental observation that the methyl proton positions are frozen at low temperatures on the time scale of the ESR experiment.

The calculations lead to a pyramidalization angle of about 40°, in agreement with earlier calculations,[6] suggesting that the rough experimental estimate of about 23°[3] is unreliable.

4. Discussion

These results indicate that methylcyclopropyl inversion is accompanied by methyl rotation. Both the methyl out-of-plane bending mode and the methyl torsional mode involve potential energy barriers, These two barriers are not independent since the rotational barrier vanishes in the transition state of the inversion mode. Because of this and because the available measurements refer to relatively high temperatures, we shall average over the methyl rotation and treat the inversion as a one-dimensional barrier problem.

To derive the effective one-dimensional barrier, we write the two-dimensional barrier in the form

$$U(q,\theta) = (Aq^4 - Bq^2 + Zq^3 \sin 3\theta)[1 + \exp(-q^2)] \quad (1)$$

where q is the out-of-plane bending coordinate and θ is the methyl rotation angle. The origin $q = \theta = 0$ is taken to be the transition state with θ halfway between the two minimum values for C_h/bm. The A and B terms determine the usual quartic potential, and the factor in square brackets corrects the curvature at the top of the barrier. The Z term introduces the asymmetry associated with methyl rotation. At temperatures where this rotation is essentially free, eq 1 can be integrated to yield the effective potential.

$$U_{eff}(q) = (Aq^4 - Bq^2)[1 + \exp(-q^2)] \quad (2)$$

The parameters A and B are chosen so as to reproduce the barrier height and width and, approximately, the curvature at the equilibrium and planar configurations. The corresponding Schrödinger equation yields eigenvalues $\epsilon_v^{\pm}$ forming closely spaced pairs below the barrier. The rate constant for a given vibrational quantum number v can be approximately expressed in terms of the pair spacing:[9]

$$k_v = 2|\epsilon_v^+ - \epsilon_v^-|/h \quad (3)$$

The thermally averaged rate constant is then given by

$$k(T) = \sum_v [k_v \exp(-\epsilon_v/k_BT)] / \sum_v [\exp(-\epsilon_v/k_BT)] \quad (4)$$

where $\epsilon_v = {}^1/_2(\epsilon_v^+ + \epsilon_v^-)$. The summation in eq 4 extends to levels above the top of the barrier with k_v corresponding to the average separation between vibrational levels in that energy region.

The rate constants calculated in this manner agree qualitatively but not quantitatively with the observed rate constants. To illustrate the discrepancy, we have reversed the procedure described above and determined empirical values of the parameters A and B so as to obtain the "best" fit to the observed rate constants, as illustrated in Figure 3. The corresponding empirical potential

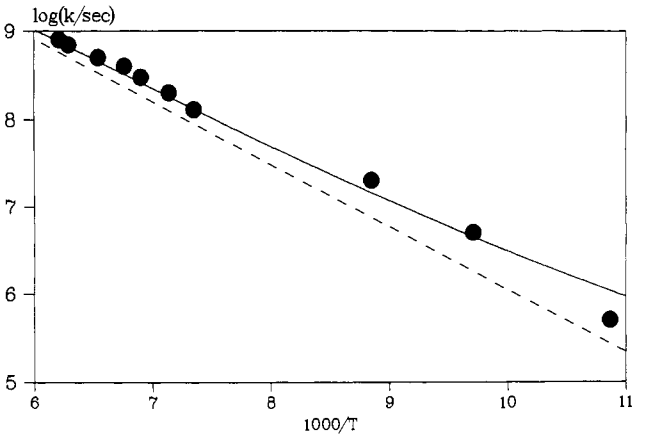

Figure 3. Comparison between observed (circles) and calculated (solid line) inversion rate constants of 1-methylcyclopropyl. The calculations are based on the effective one-dimensional potential depicted by a solid curve in Figure 4. The dashed line corresponds to calculations based on the same potential but restricted to over-the-barrier transitions, so that the separation of the two lines depicts the tunneling contribution to the inversion.

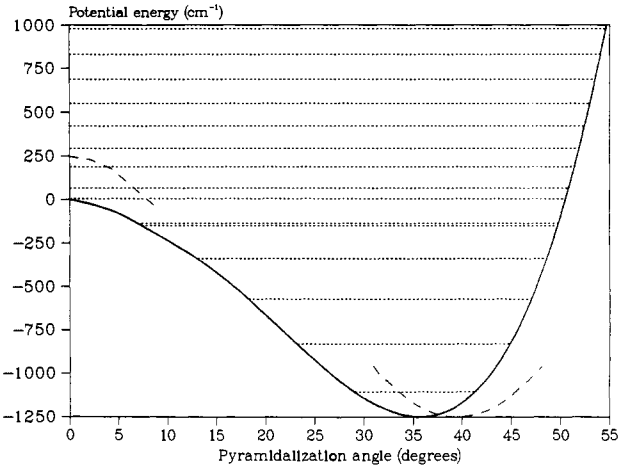

Figure 4. Comparison of the calculated (dashed) and empirical (solid) effective one-dimensional potentials for the inversion of 1-methylcyclopropyl. The energy levels (dotted) refer to the latter corresponding to eq 2 with $A = 4.205$ cm^{-1} and $B = 145$ cm^{-1}. The calculated potential refers to a fixed methyl orientation such that the inversion potential is symmetric.

is compared with the calculated potential in Table VI and Figure 4. Since the calculations are restricted to stationary points, only the energy and curvature near these points are shown. While the calculations reproduce the empirical curvatures accurately, they yield a barrier that is too high by almost 20%, a discrepancy similar to that previously observed for oxiranyl.[1]

We believe that this discrepancy reflects approximations in both the calculated and empirical potentials. In principle, one can improve the calculated potential by including electron correlation, either perturbatively, as in Møller–Plesset theory[10] or variationally through CI.[11] However, this does not seem worthwhile until the empirical barrier is calculated in terms of eq 1 rather than eq 2. Since the discrepancy disappears if we average the calculated barrier over the methyl rotation [$(1495 - 558/2)$ $cm^{-1} = 1216$ cm^{-1} compared to an empirical barrier of 1250 cm^{-1}], it follows that the rotationally averaged empirical barrier is too low. Accordingly, it overestimates the inversion rate at the lowest temperature for which data are available, in keeping with the expectation that the neglected obstruction of the methyl rotation

(9) Miller, W. H. *J. Phys. Chem.* **1979**, *83*, 960–962.

(10) Hehre, W. J.; Radom, L.; Schleyer, P. v. R.; Pople, J. A. *Ab Initio Molecular Orbital Theory*; Wiley: New York, 1986.

(11) Shavitt, I. In *Methods of Electronic Structure Theory*; Schaefer, H. F., III, Ed.; Plenum: New York, 1977.

will slow down the inversion at low temperatures. There the rotation will proceed by tunneling, which suggests that at low temperatures the inversion may show evidence of a substantial deuterium effect. Unfortunately no experimental data are available to test this suggestion.

The calculations allow an assessment of the contribution of tunneling transfer to the inversion. To this end, we have repeated the calculations including only over-the-barrier transitions. The results are represented by the broken line in Figure 3. They show that tunneling is not negligible for the inversion but becomes the dominant transfer mechanism for $T \leq 110$ K. As pointed out above, the overestimate of the transfer rate at 94 K is ascribed to the neglect of methyl rotation and should not be interpreted as support for an over-the-barrier mechanism.

The argument presented here is general and should apply to many other inversion processes involving a methyl group. These processes are expected to be slow and deuterium sensitive at low temperatures where tunneling becomes dominant. In the absence of experimental data this conclusion must take the form of a prediction.

Acknowledgment. We thank Keith Ingold for his interest in this work and numerous helpful discussions.

Registry No. Methylcyclopropyl radical, 2154-76-9.

^{51}V NMR as a Probe of Vanadium(V) Coordination to Human Apotransferrin

Alison Butler* and Hellmut Eckert

Contribution from the Department of Chemistry, University of California, Santa Barbara, California 93106. *Received January 13, 1988*

Abstract: ^{51}V NMR is a highly sensitive tool to probe the nature of the metal binding sites of human transferrin (Tf). At a field strength of 11.7 T, the two vanadium(V) binding sites in V_2-Tf are characterized by ^{51}V chemical shifts at -529.5 and -531.5 ppm versus $VOCl_3$. These shifts are assigned to the C- and N-terminal sites, respectively, based on the ^{51}V NMR spectra of vanadate addition to Fe_N-Tf and Fe_C-Tf. Tight binding of V(V) to the metal binding site is further ascertained by a linear increase of signal area with V(V) concentration up to an approximate 2:1 stoichiometry, stoichiometric displacement of protein-bound V(V) during titration with Fe(III), and the absence of the -529.5/-531.5 ppm resonance upon addition of V(V) to Fe_2Tf and Ga_2Tf. The chemical shift of the V_C-Tf resonance is independent of pH (5.8-9.0) and temperature (275-310 K), whereas the V_N-Tf resonance varies slightly (1-2 ppm) with pH and temperature. At relatively high V(V) concentrations and at high ratios of V(V)/Tf, conditions under which a large fraction of the V(V) is present as V oligomers, the ^{51}V resonance of Tf-bound V(V) is not observed, possibly owing to interference by the oligomeric species. Under conditions of tight V(V) binding, the sharpness of the protein-bound resonances is a consequence of the motional characteristics of transferrin, which place the Tf-bound vanadium(V) outside the extreme narrowing limit but within the motional narrowing limit. Several theoretically predicted consequences for an $I = {}^7/_2$ nucleus are observed experimentally, some for the first time in an aqueous protein system. (1) The observed signal intensity of transferrin-bound vanadium(V) compared to that of an equimolar aqueous vanadate sample is substantially reduced, since only one out of four spin-spin relaxation components (i.e., $+{}^1/_2 \rightarrow -{}^1/_2$ transition) is observed. (2) At 7.05 T the line width is substantially greater than at 11.7 T, and a 5-ppm upfield shift is observed which is attributed to a dynamic frequency shift. (3) The line width of Tf-bound V(V) is not affected by solvent viscosity up to 50% v/v glycerol/buffer. (4) Measurements of signal intensity as a function of pulse length reveal increased ^{51}V precession frequencies in the radio-frequency field, as frequently observed for studies of half-integer quadrupolar nuclei in the solid state. The excitation spectrum is found to be identical for V_C and V_N sites and independent of the V/Tf ratio. At small pulse angles, the fraction of the signal observed is constant and amounts to ca. 20% of that of an equimolar solution of free vanadate, in close agreement with the theoretical prediction. The present study confirms that ^{51}V NMR is a powerful tool to probe V(V) binding to apotransferrin and should also become widely applicable to characterize V(V) binding to other macromolecules.

Transferrins are glycoproteins whose primary function is to bind and transport iron. Transferrins also coordinate a wide variety of other metal ions (e.g., Cu(II), VO^{2+}, Cr(III), Ga(III), Tl(III), etc.),[1] including vanadium(V).[2-4] Human transferrin (Tf) is a single polypeptide chain with two homologous regions each of which binds one metal atom.[1] Elucidation of the similarities and differences between the two metal binding sites continues to be an area of active interest, the results of which should increase our understanding of the functional differences of the two binding sites. The X-ray crystal structure of human lactoferrin shows that the iron binding sites are separated by 42 Å and that the metal binding ligands at *both* binding sites are two tyrosine residues, one histidine residue, one aspartate residue, a H_2O (or OH^-) molecule, and an anion (CO_3^{2-} or HCO_3^-).[5] The fact that human transferrin and lactoferrin share a high degree of sequence homology (~30%),[1c] that all the metal binding amino acids in lactoferrin are conserved in human transferrin, and that much spectroscopic evidence indicates that the binding sites of lactoferrin and human transferrin are similar, suggests that the metal binding ligands are the same between transferrin and lactoferrin *and* between the two metal binding sites in human transferrin.

A wide variety of experimental results, however, suggest the two metal binding sites in human transferrin are not *equivalent*, even though the ligands of both sites may be identical. Structural differences have been inferred from the ESR spectra of the Fe(III)-,[6] VO^{2+}-,[7] Cu(II)-, and Cr(III)-bound[8] transferrin derivatives

(1) (a) Chasteen, N. D. *Adv. Inorg. Biochem.* **1983**, *58* 201. (b) Aisen, P.; Listowsky, I. *Annu. Rev. Biochem.* **1980**, *49*, 357. (c) Brock, J. H. in *Metalloproteins*; Harrison, P. M., Ed.; Verlag Chemie: Weinheim, West Germany, 1985; Part 2, p 183 and references therein.

(2) Harris, W. R.; Carrano, C. J. *J. Inorg. Biochem.* **1984**, *22*, 201.

(3) Chasteen, N. D.; Grady, J. K.; Holloway, C. E. *Inorg. Chem.* **1986**, *25*, 2754.

(4) Butler, A.; Danzitz, M. J.; Eckert, H. *J. Am. Chem. Soc.* **1987**, *109*, 1864.

(5) Anderson, B. F.; Baker, H. M.; Dodson, E. J.; Norris, G. E.; Rumball, S. V.; Waters, J. M.; Baker, E. D. *Proc. Natl. Acad. Sci. U.S.A.* **1987**, *84*, 1769-1773.

(6) Aisen, P.; Liebman, A.; Zweier, J. *J. Biol. Chem.* **1978**, *253*, 1930.

0002-7863/89/1511-2802$01.50/0